Nano Research
2024, 17(5): 4231–4243

ISSN 1998-0124 CN 11-5974/O4
https://doi.org/10.1007/s12274-023-6292-8

Review Article

Odd-even effects in the structure and properties of aryl-substituted aliphatic self-assembled monolayers

Piotr Cyganik[1], Andreas Terfort[2], and Michael Zharnikov[3] (✉)

[1] *Jagiellonian University, Faculty of Physics, Astronomy and Applied Computer Science, Smoluchowski Institute of Physics, Łojasiewicza 11, 30-348 Kraków, Poland*
[2] *Institut für Anorganische und Analytische Chemie, Universität Frankfurt, Max-von-Laue-Straße 7, 60438 Frankfurt, Germany*
[3] *Applied Physical Chemistry, Heidelberg University, Im Neuenheimer Feld 253, 69120 Heidelberg, Germany*

Received: 23 September 2023 / **Revised:** 17 October 2023 / **Accepted:** 26 October 2023

ABSTRACT

Self-assembled monolayers (SAMs) represent an important tool in context of nanofabrication and molecular engineering of surfaces and interfaces. The properties of functional SAMs depend not only on the character of the tail groups at the SAM-ambient interface, but are also largely defined by their structure. In its turn, the latter parameter results from a complex interplay of the structural forces and a variety of other factors, including so called odd-even effects, viz. dependence of the SAM structure and properties on the parity of the number (odd or even) of individual building blocks in the backbone of the SAM constituents. The most impressive manifestation of the odd-even effects is the structure of aryl-substituted alkanethiolate SAMs on Au(111) and Ag(111), in which, in spite of the fact that the intermolecular interaction is mostly determined by the aryl part of the monolayers, one observes a pronounced dependence of molecular inclination and, consequently, the packing density of the SAM-forming molecules on the parity of number of methylene units in the alkyl linker. Here we review the properties of the above systems as well as address fundamental reasons behind the odd-even effects, including the existence of a so-called bending potential, which is frequently disregarded in analysis of the structure-building forces. The generality of the odd-even effects in SAMs is additionally supported by the recent data for SAMs on GaAs, scanning tunneling microscopy data for SAMs on Ag(111), and the data for the monolayers with selenolate and carboxyl anchoring groups on Au(111) and Ag(111). The implications of these effects in terms of the control over the packing density and orientation of the tail groups at the SAM-ambient interface, structural perfection, polymorphism, temperature-driven phase transitions, and SAM stability toward such factors as ionizing radiation, exchange reaction, and electrochemical desorption are discussed. These implications place the odd-even effects as an important tool for the design of functional SAMs in context of specific applications.

KEYWORDS

self-assembled monolayers, molecular films, surface and interface engineering, odd-even-effects

1 Introduction

Self-assembled monolayers (SAMs) are an important part of modern nano- and biotechnology, providing a means to form well-defined organic surfaces, a versatile tool to modify surface and interfacial properties, and a platform for specific applications, such as sensors, molecular electronics, carbon nanomembranes, lithography, and more [1–14]. SAM-forming molecules are usually rod-shaped and consist of three essential parts, viz. anchoring group, making a covalent-like bonding to the substrate, tail group, comprising the SAM-ambient interface, and molecular backbone, connecting the anchoring and tail groups and driving the process of self-assembly by intermolecular interactions. All these parts can be flexibly and independently selected to adjust for the identity of the substrate and the desired function of a particular SAM. A specific combination of these parts as well as the choice of the substrate define the structure of a SAM, which is of primary importance for the SAM properties and the range of possible applications. In most cases, dense molecular packing and possibly upright molecular orientation are desirable, to achieve the maximal effect of the molecular assembly, e.g., in terms of substrate protection, maximal density of functional tail groups, or favorable orientation of the molecular dipole moments. Optimization of these parameters relies on a complex interplay of structural forces, including the interactions between the substrate and anchoring groups, between the molecular backbones (chain-chain), and between the tail groups, as well as possible sterical constraints in case of bulky tail groups. There are, however, some additional factors, which are especially relevant for such archetypical and frequently used SAM systems as alkanethiolate monolayers on Au(111) and Ag(111) substrates [2–4, 15]. The combination of an alkanethiolate linker and a unsubstituted or substituted aryl moiety within a hybrid backbone, which can be seen both as a substitution at an alkanethiolate or as an introduction of an alkyl linker in between the aryl part and the thiolate group, results generally in a non-trivial structural behavior, termed as odd-even effects [16–18]. In spite of the fact that the intermolecular interaction (E_{inter}) is then mostly dominated by the aryl part of the monolayers, there is a

Address correspondence to Michael.Zharnikov@urz.uni-heidelberg.de

清華大學出版社 Tsinghua University Press Springer

pronounced dependence of molecular inclination and, consequently, the packing density of the SAM constituents on the parity of the number (n) of methylene units in the alkyl linker. The present paper reviews the properties of the respective systems as well as addresses the fundamental reasons behind the odd-even effects, including the existence of a so-called bending potential (E_{bend}), which is frequently neglected in analysis of the structure-building forces. The generality of the odd-even effects in SAMs is additionally supported by recent data for GaAs substrates, scanning tunneling microscopy data for Ag(111), and data for the monolayers with selenolate and carboxyl anchoring groups on Au(111) and Ag(111). The implications of these effects on the packing density and orientation of the tail groups at the SAM-ambient interface, structural perfection, polymorphism, temperature-driven phase transitions, SAM stability toward ionizing radiation, exchange reactions, and electrochemical desorption are discussed. These implications place the odd-even effects not only as an interesting phenomenon from the viewpoint of fundamental research but also as an important tool for the design of functional SAMs in context of specific applications.

2 Origin and manifestation of the odd-even effects

The first hints that the introduction of an aliphatic linker between the thiolate anchoring group and an aryl backbone can greatly influence the structure of aromatic SAMs, resulting in some cases in its significant improvement, were obtained in the early studies involving SAMs of phenyl-, biphenyl, and terphenylthiols on Au(111) [19–23]. It was found that the introduction of a single methylene group between the aryl moiety and thiol group significantly enhances the ability of the molecules to form ordered monolayers and lead to an increase in the packing density [19–23]. In a parallel study of a family of phenyl-substituted, long-chain alkanethiolate SAMs on Au(111), only minor odd-even behavior of some structural fingerprint characteristics was recorded, although an odd-even variation of the wetting properties for several liquids was found [24].

The first systematic study of the odd-even effects in aryl-substituted alkanethiolate SAMs was performed for the monolayers of ω-(4′-methyl-biphenyl-4-yl)-alkanethiols (CH_3-C_6H_4-C_6H_4-$(CH_2)_n$-SH (MeBPnS; n = 1–6; Me = CH_3)) formed on Au(111) and Ag(111) substrates under the standard conditions (immersion into ethanolic precursor solution at room temperature) [16, 17]. These systems (Fig. 1(a)) were studied by a combination of several complementary experimental techniques, including X-ray photoelectron spectroscopy (XPS), near-edge X-ray absorption fine structure (NEXAFS) spectroscopy, and infrared reflection-absorption spectroscopy (IRRAS). According to the NEXAFS spectroscopy data (Figs. 1(b) and 1(c)), the average tilt angles of the biphenyl groups in the MeBPnS SAMs vary in an odd-even fashion, showing smaller values for n = odd and larger values for n = even on Au and the opposite behavior on Ag. The changes in the molecular inclination were accompanied by alternating changes in the packing density, as evidenced by the intensity ratios of the XPS signals stemming from the SAMs and the substrate, respectively (Figs. 1(d) and 1(e)). Higher and lower packing densities were observed for n = odd and n = even, respectively, on Au; the opposite behavior was recorded on Ag.

The odd-even variation of the packing density was additionally verified for Au(111) by scanning tunneling microscopy (STM) [26, 27]. Representative images for n = odd (MeBP3S) and n = even (MeBP4S) systems are presented in Figs. 2(a) and 2(b), respectively. According to these images, the structures and packing densities of the respective SAMs are distinctly different. The unit cell of the MeBP3S SAM, representative of the other MeBPnS monolayers with n = odd as well, is described by an oblique $(2\sqrt{3} \times \sqrt{3})R30°$ structure and contains two molecules. In contrast, the MeBP4S SAM is described by a much larger, rectangular $(5\sqrt{3} \times 3)$ structure with eight molecules per unit cell, recorded for the other MeBPnS monolayers with n = even as well. Significantly, the area occupied per molecule (molecular footprint) for n = odd (21.6 Å^2) is smaller than that for n = even (27.05 Å^2) by about 25% [27], correlating thus perfectly with the results of the spectroscopic characterization, described above [16, 17]. Note that along with the linear dichroism in NEXAFS spectroscopy and the intensity of the C 1s and substrate signals in the XPS spectra, a variety of other fingerprint features associated with the structure of the MeBPnS SAMs, such as intensities of the characteristic IR modes, ellipsometric thicknesses, parameters of the photoemission peaks, wetting properties, etc., exhibited odd-even behaviors correlating perfectly with the structural changes [16, 17, 28].

The explanation of the odd-even behavior is illustrated in Fig. 3. Two factors are of primary importance. First, the substrate–S–C unit is obviously not a free-moving joint, which might adapt any arbitrary angle to balance the structural forces in the given SAM. Rather, there is a preferable geometry of this joint, which can be

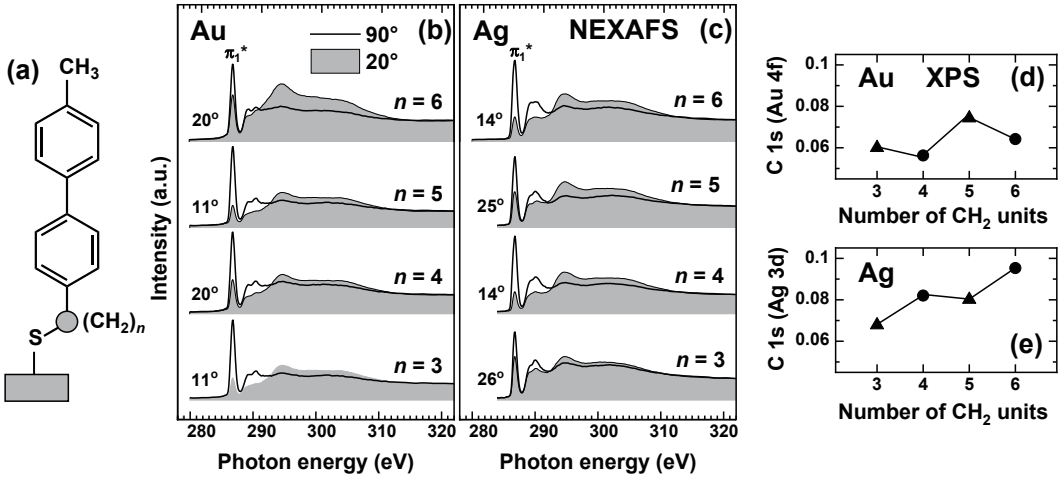

Figure 1 (a) Schematic of the MeBPnS structure after its chemisorption onto the substrate. NEXAFS spectra of the MeBPnS SAMs on (b) Au and (c) Ag acquired at X-ray incidence angles of 90° (bold solid lines) and 20° (shadowed spectra). The intensity difference at the position of the π_1^* resonance, described as linear dichroism in X-ray absorption, is a fingerprint of molecular orientation and orientational order [25]. The derived tilt angles of the biphenyl groups with respect to the surface normal are given at the respective spectra. (d) and (e) XPS-derived intensity ratios as functions of n. Reproduced (adapted) with permission from Ref. [16], © The Royal Society of Chemistry 2000.

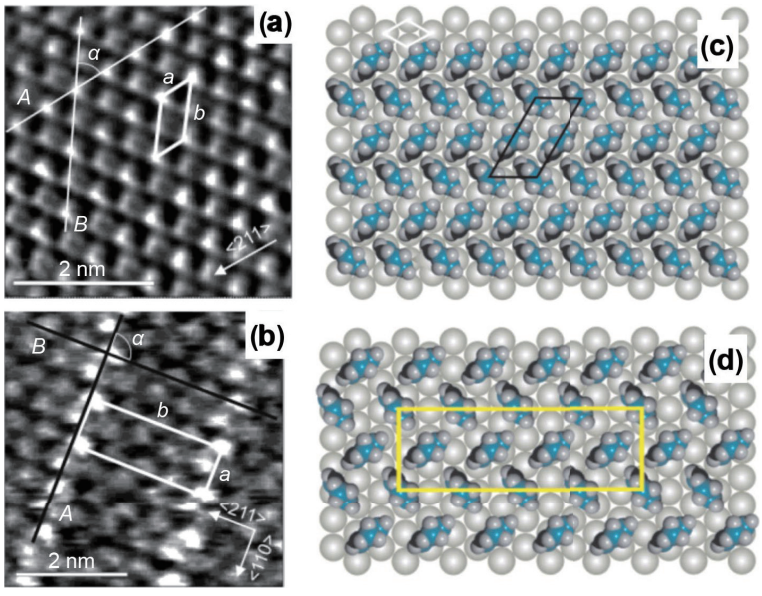

Figure 2 STM images of the (a) MeBP3S and (b) MeBP4S. SAMs on Au(111) along with the respective structural models for (c) MeBP3S and (d) MeBP4S. The unit cells are marked (see text for details). The dimensions of the unit cells were determined with the help of the height profiles (not shown) along the lines A and B in (a) and (b). Adapted with permission from Refs. [26, 27], © American Chemical Society 2003 and 2004, respectively.

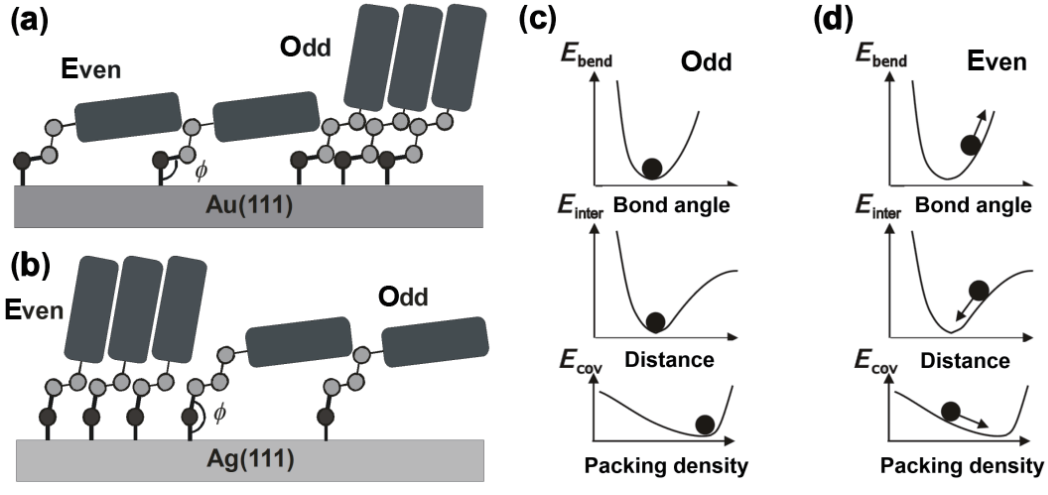

Figure 3 Schematic explanation of the odd-even effects in the aryl-$(CH_2)_n$-S SAMs on (a) Au(111) and (b) Ag(111), by the example of MeBP2S and MeBP3S; the biphenyl group is schematically drawn as a rounded rectangle. Balance of the structural forces associated with the E_{bend}, intermolecular interaction (E_{inter}), and coverage (E_{cov}) for (c) n = odd and (d) n = even on Au(111). The parameters are the substrate–S–C bond angle, the average distance between molecules, and the molecular packing density. Adapted with permission from Refs. [28, 32], © American Chemical Society 2001 and 2006, respectively.

tentatively associated with an sp^3 bonding configuration of the S atom on Au(111) and an sp configuration of this atom on Ag(111) [16], with the difference related probably to the different energetics of S–Au and S–Ag bonds [29] and/or involvement of Au adatoms on Au(111) [30, 31]. The respective substrate–S–C angles are ~ 104° and ~ 180°, giving a specific orientation to the adjacent CH_2 segment. This orientation is then transferred to the aryl unit by the alkyl linker, which tends to adopt the thermodynamically favorable all-*trans* conformation—the second important factor in the context of the odd-even effects. As seen in Figs. 3(a) and 3(b), in which the extent of these effects is somewhat exaggerated, the combination of the preferred bond angle and all-*trans* conformation of the alkyl linker results in an upright orientation of the aryl groups for n = odd on Au and n = even on Ag. In contrast, strongly inclined orientation of these groups occurs for n = even on Au and n = odd on Ag, hindering a dense molecular packing. Of course, the substrate–S–C joint is not absolutely rigid, but can change its geometry to some extent, working against the so-called bending potential, which reflects the optimal anchoring geometry and has its minimum at a certain substrate–S–C angle, specific for the particular substrate (see the top panels in Figs. 3(c) and 3(d)). Thus, the bending potential contributes to the balance of the "conventional" structural forces, affecting the resulting SAM structure. There are, however, two distinctly different ways how such a combination occurs depending on the parity of n [32], as schematically illustrated in Figs. 3(c) and 3(d) for the case of Au(111). The general tendencies of monomolecular assemblies are to maximize the packing density (given by the number of Au–S bonds per area unit) and to optimize the intermolecular interactions. All this can be achieved easily in the case of n = odd, in which the bending potential, entering the force balance in a cooperative fashion, does not prevent dense molecular packing and allows for most optimal molecular interaction (Fig. 3(c)) and realization of a thermodynamic energy minimum. In contrast, for n = even, the bending potential contributes to the force balance in a competitive fashion, preventing a tight molecular packing and optimal intermolecular interaction (Fig. 3(d)), so that an energetic state less favorable than for n = odd is realized. As a result, the Au–S–C joint is noticeably strained, which is in particular reflected by the characteristic binding energies of the anchoring

groups as measured by XPS [28, 33] as well as by some other properties, as will be discussed in further sections of this article. Note that all arguments suitable for Au(111) in relation to Fig. 3(a) are also applicable to Ag(111), with the reverse relation of the structural effects to the parity of *n*. Note also that the inclination of the aryl group is probably not the only orientational parameter exhibiting odd-even behavior. It is possible that also the torsion (twist) of the entire aryl group with respect to the tilt plane or torsion between the two phenyl rings in the biphenyl moiety exhibit an odd-even variation as well. Such torsion variation is even sometimes considered as the major structural change [34], which is, however, rather unlikely since the odd-even effects are also recorded for acene groups, featuring annelated aromatic rings (see below).

3 Generality of the odd-even effects

Whereas the odd-even effects have been first systematically observed and rationalized for MeBPnS SAMs on Au(111) and Ag(111) [16, 17, 26–28], as discussed in the previous section, they were later reported for a broad variety of other aryl groups, such as terphenyl [33, 35, 36], perfluoroterphenyl [37], aceneoxazole [38], perfluoroanthracene [39], cyano-biphenyl [40, 41], and azobenzene [42]. So far, these effects were observed with all aryl group tried, except for the specific molecular geometries discussed in the next section.

Moreover, the odd-even effects were recorded not only for the thiolate anchoring group and Au(111) and Ag(111) substrates but also for the selenolate anchoring group, capable as well to bind functional molecules to these substrates. Note that sulfur and selenium have similar valence electron configurations and are neighbors in the 16th group of the periodic table, so that it is only logical that the respectively anchored SAMs exhibit similar properties.

Representative data for the SAMs of (methyl-biphenylyl) alkaneselenolates (MeBPnSe) on Au(111) and Ag(111) are shown in Fig. 4. As seen in Figs. 4(a) and 4(b), both the effective SAM thickness and the inclination of the biphenyl groups exhibit distinct odd-even behavior, with the same relation of these parameters to the parity of *n* as for the analogous monolayers with the thiolate anchoring group (see Fig. 1) [43, 45]. Complementary STM data for the MeBP3Se and MeBP4Se SAMs on Au(111) are presented in Figs. 4(c) and 4(d), respectively, representative of the entire MeBPnSe series [44]. The respective structural models and schematic sketches of the structures are shown in Figs. 4(e) and 4(g) for MeBP3Se and Figs. 4(f) and 4(h) for MeBP4Se [44]. According to the STM data, the unit cell of MeBPnSe SAMs with *n* = odd can be described as close to a commensurate oblique $(2\sqrt{3} \times \sqrt{3})R30°$ structure with two molecules per unit cell (Fig. 4(c)). In contrast, the molecular arrangement in MeBPnSe SAMs with *n* = even can be described by an irregular anisotropic expansion of the above structure along its shorter unit cell vector (Figs. 4(f) and 4(h)). Due to the irregularity, the respective unit vector in the direction of the expansion cannot be defined but, as the result of this expansion, the SAMs with *n* = even are characterized by about 22%–28% lower packing density than those with *n* = odd. Thus, the extent of the odd-even effects in the MeBPnSe SAMs is close to that in the analogous MeBPnS monolayers (~ 25%; see the previous section).

Interestingly, the structures of the MeBPnSe and MeBPnS SAMs with *n* = odd are nearly identical, resulting from the favorable balance of the structure-building interactions (see Fig. 3(c)). In contrast, the structures of the MeBPnSe and MeBPnS SAMs with *n* = even are distinctly different, viz. the irregular expanded, one-dimensional (1D)-ordered oblique $(2\sqrt{3} \times \sqrt{3})R30°$ arrangement (MeBPnSe) versus the two-dimensional (2D)-ordered, rectangular $(5\sqrt{3} \times 3)$ structure (MeBPnS). Apart from the competitive balance of the structure-building interactions (see Fig. 3(d)), the key factor behind this difference is significant mobility of the gold atoms in the topmost layer of the substrate induced by the selenium atoms [44], resulting in a higher adaptivity of the film structure to the specific balance of the relevant interactions. The bonding between Se and Au substrate is stronger than that for S, so that the anchoring Se group are capable of dragging the topmost gold atoms to adapt a structure most suitable for the given molecular assembly [46–48]. This drag occurs however on the expense of bonding energy between the atoms in the topmost and penultimate layers of the substrate, so that there is an accumulation of stress increasing with the size of the restructured domains. Consequently, these domains are limited to a certain size, resulting in the irregularity of the overall molecular structure [44].

Significantly, the odd-even effects are not limited to the Au(111) and Ag(111) substrates, but are also characteristic of semiconductor materials, such as GaAs. Whereas well defined SAMs can be prepared on the different low-index surfaces of GaAs using the thiolate anchoring group [50], the odd-even effects were only tested for the GaAs(001) face. Both methyl-biphenyl- (MeBPnS) and terphenyl-substituted (TPnS) molecules were investigated and a similar behavior was recorded as with Au(111)

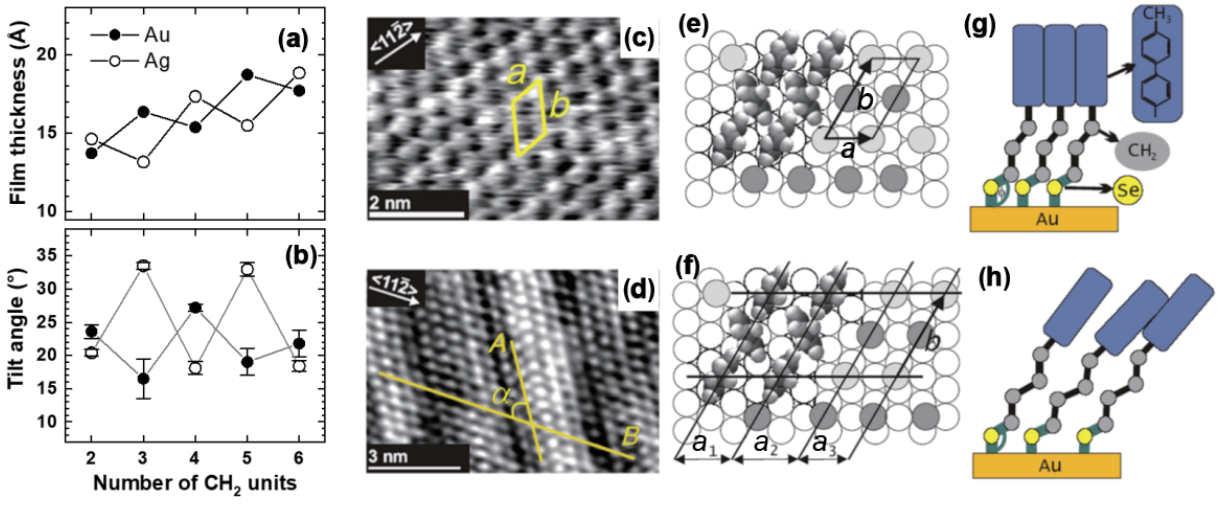

Figure 4 (a) Effective film thickness and (b) average tilt angle of the biphenyl groups with respect to the surface normal in the MeBPnSe SAMs on Au(111) and Ag(111). STM images of the (c) MeBP3Se and (d) MeBP4Se on Au(111) along with ((e) and (f)) the respective structural models and ((g) and (h)) schematics of the molecular organization. Adapted with permission from Refs. [43, 44], © American Chemical Society 2007 and 2008, respectively.

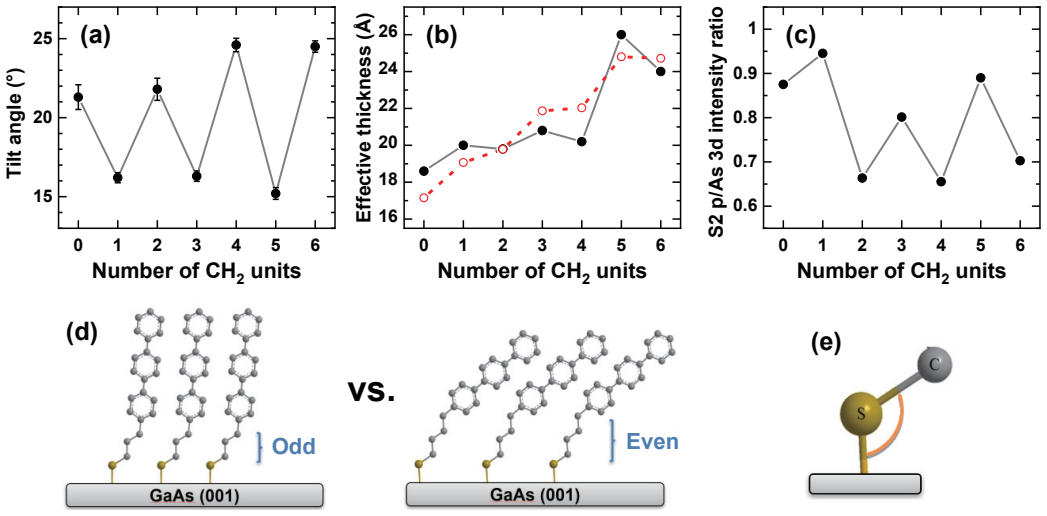

Figure 5 (a) Average tilt angle of the terphenyl groups with respect to the surface normal, (b) effective film thickness derived from the XPS (black circles) and NEXAFS (red circles) data, and (c) S 2p /As 3d intensity ratio for the TPnS SAMs on GaAs(001). (d) Schematic of the odd-even effects in the system. (e) Optimal geometry of the GaAs–S–C joint. Adapted with permission from Ref. [49], © American Chemical Society 2013.

[49, 51]. Representative data for the latter system are shown in Fig. 5. There is a distinct odd-even behavior both in the orientation of the terphenyl groups (Fig. 5(a)) and in the packing density in the SAMs, expressed by their effective thickness (Fig. 5(b)) and the S 2p/As 3d intensity ratio (Fig. 5(c)). Interestingly, as shown in Fig. 5(d), the smaller molecular inclination and the higher packing density are observed for the SAMs with n = odd, which mimics the behavior of the analogous systems on Au(111) (see Fig. 3(a) and Ref. [35]). Consequently, the alkanethiolate SAMs on GaAs(001) feature a similar bonding configuration of the S atom, with an optimal bonding angle of ~ 105° (Fig. 5(e)).

Note that the odd-even effects are not necessarily limited to the GaAs(001) substrate but can also occur for other semiconductor materials, such as InP and Si, which, however, have not been specifically studied so far in the given context. Also, metal substrates other than Au(111) and Ag(111) may exhibit the odd-even effects, which can be a subject of dedicated future research.

4 Geometry-related exceptions

As mentioned above, the odd-even effects have been observed for all aryl groups tried. However, the situation is not entirely straightforward in some specific cases, as shown by the example of anthracene-terminated molecules (Fig. 6). The direct attachment of anthracene (Ant) to the alkyl linker cannot occur along the long axis because of the specific structure of acenes. Consequently, the attachment has to take place asymmetrically, resulting in an additional degree of freedom in form of the rotatability of the anthracene group within a large space angle, as schematically illustrated in Fig. 6(a) for the respective Ant-n-S SAMs on Au(111). This rotation permits the adoption of an almost upright orientation of the aromatic part regardless of the parity of n as shown in Fig. 6(a) for n = 2 (even) and n = 3 (odd). Indeed, both the inclination of the anthracene groups, given by the orientation of the respective π* orbitals (Fig. 6(b)) and the effective thickness of the SAMs (Fig. 6(c)) do not exhibit pronounced and systematic odd-even effects [52]. Nevertheless, the odd-even-effects can be recovered for the (anthr)acene system, if it becomes annelated with an oxazole (Ox) unit (Fig. 6(d)), which allows a (pseudo)symmetrization by permitting the substitution along the long axis, as shown in Figs. 6(e) and 6(f) for the respective AntOx-n-S SAMs [38].

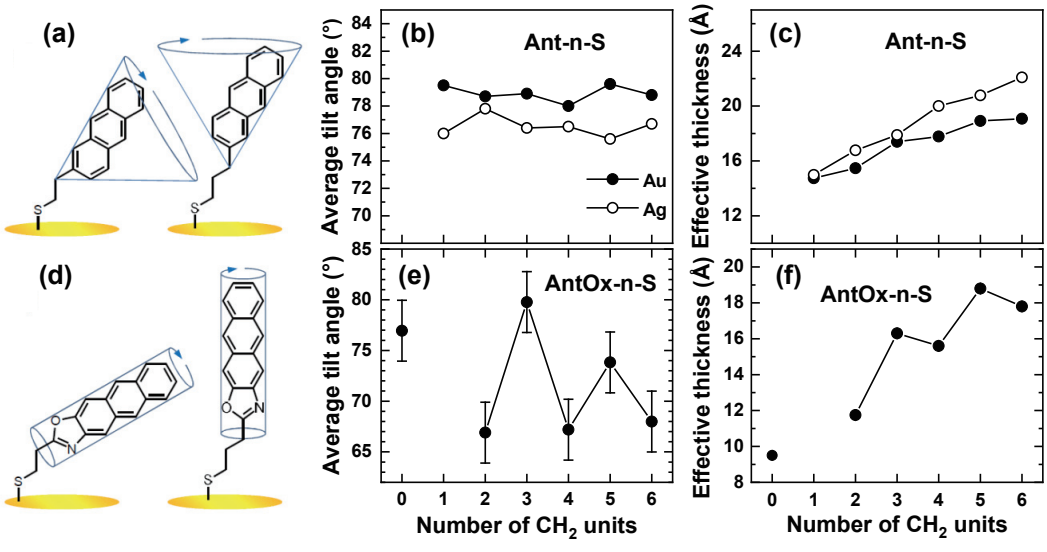

Figure 6 Schematic of the behavior of the (a) Ant-n-S and (b) AntOx-n-S SAMs on Au(111) and Ag(111) (for Ant-n-S only) along with ((b) and (e)) the average tilt angle of the π* orbitals of the anthracene groups with respect to the surface normal and ((c) and (f)) the effective thickness for these monolayers. Note that the π* orbitals of the anthracene group are oriented perpendicular to the plane of this group. Adapted with permission from Refs. [52, 38], © American Chemical Society 2011 and 2019, respectively.

5 Polymorphism

The structure of aryl-substituted alkanethiolate and alkaneselenolate SAMs with n = even on Au(111) and with n = odd on Ag(111) results from a balance of several competitive factors, as schematically shown in Fig. 3(d). This can lead to metastable structures, governed probably by kinetic factors, which can be easily transformed into more stable ones by post-deposition annealing. A representative example in this context is provided by the MeBP4S and MeBP6S SAMs on Au(111) [32, 53], with the data for the MeBP4S case shown in Fig. 7. As mentioned above (section 2), preparation of this monolayer at the standard conditions (room temperature, 1 mM solution) results in the formation of a rectangular $5\sqrt{3} \times 3$ structure with eight molecules per unit cell and an area per molecule of 27.05 Å^2 (Fig. 7(a)). However, post-deposition annealing of this SAM at 373 K for 15 h leads to the transformation of the $5\sqrt{3} \times 3$ structure, denoted as α-phase, into a $6\sqrt{3} \times 2\sqrt{3}$ arrangement, denoted as β-phase (Fig. 7(b)). The unit cell of the latter phase also contains eight molecules but is significantly larger, so that the area per molecule becomes 32.4 Å^2. A further structural transformation occurs upon annealing for 15 h at a slightly higher temperature of 383 K. It corresponds to the emergence of a new, $2\sqrt{3} \times \sqrt{13}$ structure with four molecules in the unit cell and an area per molecule of 25.2 Å^2, denoted as γ-phase (Fig. 7(c)). The structures of all three phases are additionally visualized in Fig. 7(d). The different structural arrangements and different molecular packing densities of these phases are accompanied by different molecular orientations of the SAM-forming molecules, as illustrated in Figs. 7(e) and 7(f) for the α- and β-phase. The respective NEXAFS spectra exhibit distinctly different extents of linear dichroism (intensity difference at the positions of characteristic resonances upon variation of the incidence angle of the primary X-rays). The analysis of these data suggests that the molecules in the α- and β-phases not only feature different tilt angles with respect to the surface normal but have also different twist angles (torsion), describing the rotation of the entire biphenyl group with respect to the tilt plane [32].

Note that polymorphism in aryl-substituted aliphatic SAMs was not only reported for thiolates but for selenolates as well, viz. for the MeBPnSe (n = 2–6) monolayers on Au(111) [54]. Whereas the SAMs with n = odd exhibited only a single phase, those with n = even formed two or three different coexisting phases, including the one observed at room temperature. The latter phase (α-phase) featured 1D-character and an area per molecule of 26–27.7 Å^2. In contrast, the new phases had 2D-character and were either commensurate (β-phase, rectangular $5 \times 2\sqrt{3}$) or incommensurate (γ-phase, oblique $2\sqrt{3} \times 1.2\sqrt{3}$) with the Au(111) substrate, featuring an area per molecule of 37.5 and 26 Å^2, respectively [54]. Interestingly, the phase transition to the new phases took place already at slightly elevated temperature of incubation (333 K) confirming much higher mobility of MeBPnSe molecules on Au(111) surface compared to MeBPnS for which post-deposition annealing at noticeably higher temperature was needed to induce the phase transitions (see above).

6 Carboxylate-anchored SAMs

As shown recently [55], odd-even effects in aryl-substituted aliphatic monolayers are not limited to the thiolate- and selenolate-anchored films, but are also characteristic of SAMs of aryl-substituted fatty acids on Ag(111). For these films, the bonding to the substrate occurs via the carboxylate (COO^-) anchoring group. Representative data for the case of biphenyl-substituted carboxylates (BPnCOO) are presented in Fig. 8. Accordingly, the effective film thickness (Fig. 8(a)) and the area per molecule (Fig. 8(b)) exhibit distinct zig-zag behavior, with the higher thickness and molecular density for n = even and the lower thickness and molecular density for n = odd. The respective STM images show a highly ordered molecular structure for n = even (Fig. 8(c)) and a coexistence of amorphous (α) and quasi-ordered (β) phases for n = even (Fig. 8(d)). The explanation of this behavior is illustrated in Figs. 8(e)–8(h). Similar to the thiolate and selenolate case, the key factors are (i) the optimal upright geometry of the substrate–OOC joint with an optimal bonding angle across this joint of ~ 180° (see Fig. 8(e)) and (ii) favorable all-trans conformation of the alkyl linker, transferring the geometry of the substrate–OOC joint to the attached biphenyl moiety, which follows the orientation of the topmost CH_2 segment. Accordingly, n = even corresponds to optimal adsorption geometry, allowing for upright orientation of the terminal biphenyl groups and, consequently, for dense molecular packing and long-range structural order (Fig. 8(e)). In contrast, the BPnCOO films with n = even feature large inclination of the biphenyl groups, hindering a dense molecular packing and good orientational order and resulting in a liquid-like structure. Note that the observed odd-even effects for the BPnCOO SAMs on Ag are generally consistent with the tentative model presented in Figs. 3(c) and 3(d), which, importantly, is based on competition of only enthalpic contributions to the energetics of the systems discussed in the previous sections. In contrast, for the BPnCOO monolayers, the ordered and liquid-like

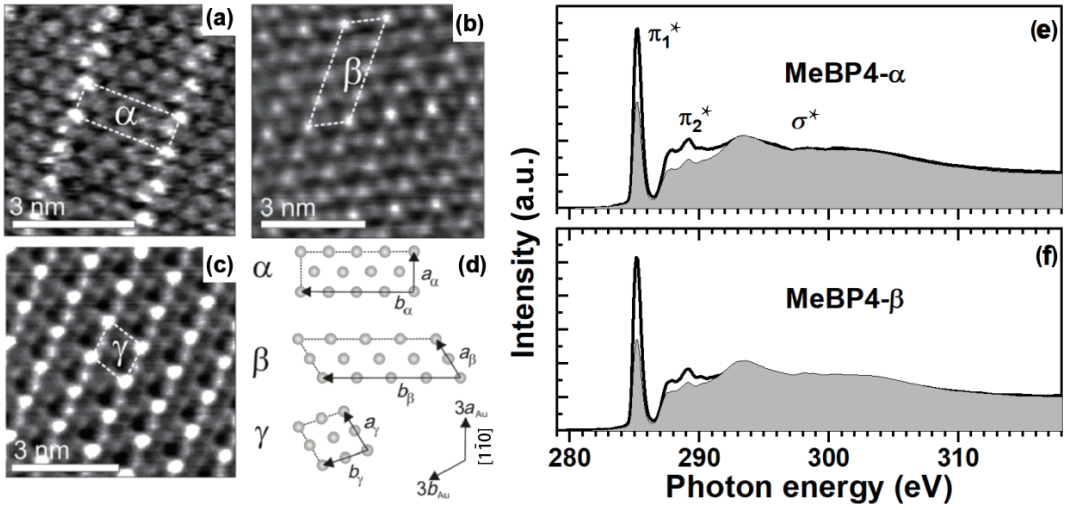

Figure 7 High-resolution STM images of the MeBP4S SAM on Au(111) showing the structures of the (a) α, (b) β, and (c) γ phases. (d) Schematic drawings of the respective unit cells. ((e) and (f)) NEXAFS spectra of the α and β phases of the MeBP4S SAM acquired at X-ray incidence angles of 90° (bold solid lines) and 30° (shadowed). The most characteristic absorption resonances are marked. Adapted with permission from Ref. [32], © American Chemical Society 2006.

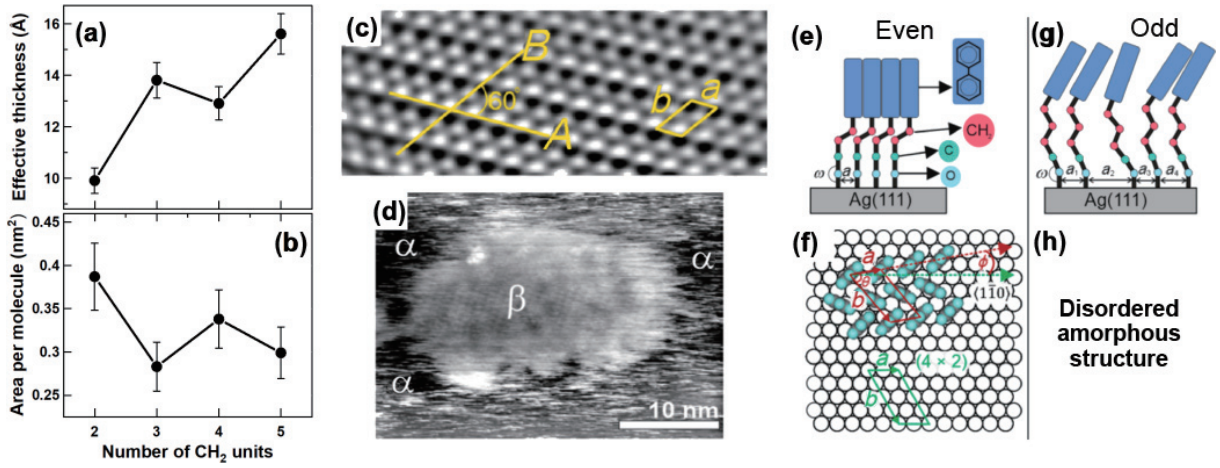

Figure 8 (a) Effective film thickness and (b) area per molecule for the BPnCOO SAMs on Ag(111), along with STM images of the (c) BP2COO and (d) BP3COO monolayers, and the schematic drawing of the molecular arrangement for ((e) and (f)) n = even and ((g) and (h)) n = odd under the reasonable assumption of an optimal substrate–OOC bonding angle of ~ 180° in (e) and (g). The unit cell of the BP2COO structure is marked in (c) and drawn in (f). The amorphous (α) and quasi-ordered (β) phases are marked in (d). Adapted with permission from Ref. [55], © American Chemical Society 2017.

structures obtained for n = even and n = odd, respectively, indicate certain entropic contributions which are, apparently, still of minor importance considering that the observed odd-even effects are very similar to those in the thiolate and selenolate SAMs where such contributions are presumably quite small. These considerations additionally confirm the validity of the proposed model where enthalpic contributions, such as coverage, intermolecular interactions and the bending potential, play a dominant role for the odd-even effects.

7 Odd-even effect related properties

The significant variation of the packing density, orientational order, molecular orientation, and structure of aryl-substituted aliphatic SAMs, associated with the parity of n, affects their properties. This includes in particular the sensitivity of these monolayers to electron irradiation, which is an important issue in context of SAM-based lithography and carbon nanomembrane (CNM) fabrication [6, 13, 56] Typical reactions during electron exposure are cleavage of intramolecular C–H and C–C bonds as well as S–substrate bonds, followed by the formation of intermolecular C–C bonds (crosslinking), and rearrangment of the residual molecular backbones [56]. All these processes are accompanied by molecular reorientation. Representative data are shown in Fig. 9, in which the evolution of several fingerprint parameters of the MeBPnS SAMs (n = 0, 1, 4, 5 and 12) on Au(111) after their exposure to electron irradiation (10 eV; 8 mC/cm^2) are presented. Accordingly, the intensities of the characteristic IR modes for both the biphenyl group (Fig. 9(a)) and terminal methyl groups (Fig. 9(b)) decrease much less for the SAMs with n = odd than for those with n = even. A similar situation occurs also for the linear dichroism in X-ray absorption (Fig. 9(c)), which represents a measure of the orientational order in the films. Thus, the more densely packed and better oriented SAMs with n = odd are more robust and less sensitive to electron irradiation compared to their counterparts with n = even. Interestingly, the behavior of the biphenylthiolate SAMs without the aliphatic linker (n = 0) is similar to that for n = even, which is a further evidence that the introduction of a proper linker between the aryl group and the anchoring group improves the quality and robustness of the SAMs.

A similar behavior with respect to electron irradiation was also observed for the BPnCOO SAMs on Ag(111) [58]. The experimental data for these systems show a clear odd-even behavior for characteristic electron-irradiation-induced processes, such as desorption, cross-linking within the SAM matrix, and damage of the anchoring groups. The more densely packed and better ordered SAMs with n = even (see section 6) exhibit lower extent of the above processes compared to those with n = odd. Considering that electron-irradiation-induced crosslinking of aromatic matrix is the most important process in the context of fabrication of SAM-derived CNMs [6], these results demonstrated also a way for controlling thickness and purity of such nanomembranes, which are the key parameters for determining the range of their applications [59].

A variety of further examples for the influence of the odd-effects on diverse properties is provided in Fig. 10. First, the relative stability of the MeBPnS (Fig. 10(a)) and MeBPnSe (Fig. 10(b)) SAMs on Au(111) with respect to the molecular exchange is illustrated [60]. For this purpose, these SAMs were immersed

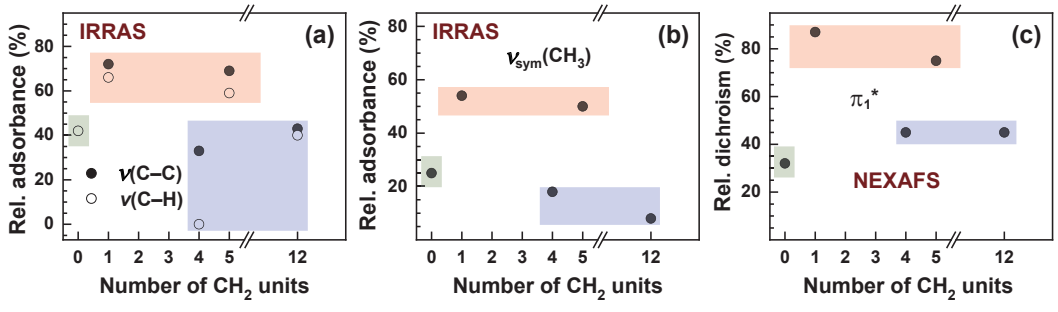

Figure 9 Evolution of fingerprint parameters of the MeBPnS SAMs on Au(111) after their exposure to electron irradiation: (a) intensities of the characteristic ν(C–C) and ν_{ip}(C–H) bands associated with the biphenyl group; (b) intensities of the characteristic $\nu_{sym}(CH_3)$ band of the terminal methyl group; and (c) extent of the linear dichroism associated with the π_1^* resonance of the biphenyl moiety (NEXAFS spectroscopy) [57]. All values are normalized to those of the pristine SAMs. The values for the SAMs with n = odd, n = even, and n = 0 are shadowed in red, blue, and green, respectively.

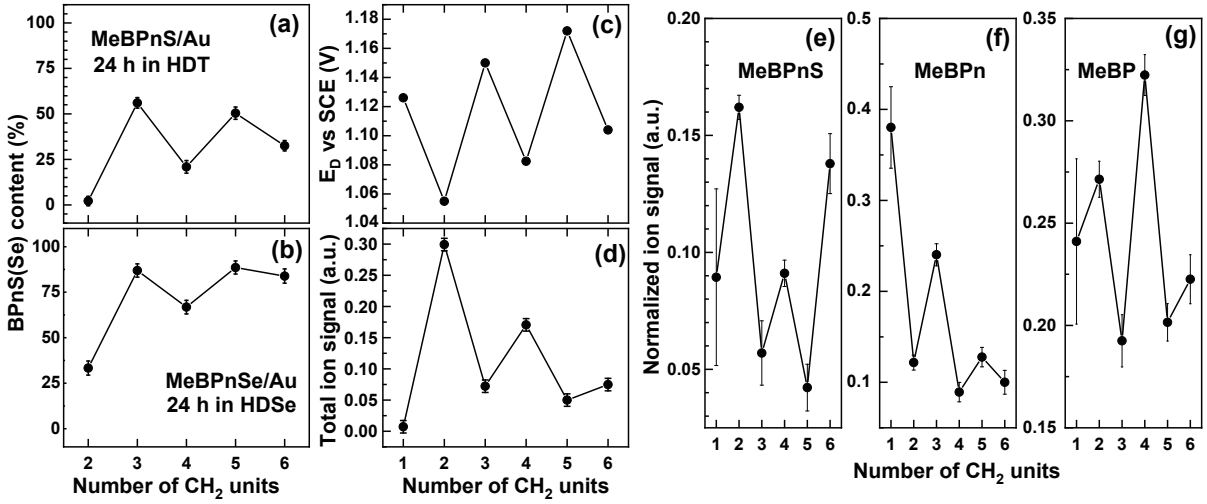

Figure 10 Fingerprint parameters for the response of the MeBPnS SAMs on Au(111) to external factors as functions of *n*. (a) Residual portion of the MeBPnS molecules after the exposure of the respective MeBPnS SAMs to a HDT solution. (b) Residual portion of the MeBPnSe molecules after the exposure of the MeBPnSe SAMs to a HDSe solution. (c) Electrochemical desorption peak potential for the MeBPnS SAMs in 0.5 M aqueous KOH. ((d)–(g)) S-SNMS ion signals from the MeBPnS SAMs during 15 keV Ar^+ ion irradiation: (d) total signal, (e) molecular signal (MeBPnS), (f) desulfurized fragment signal (MeBPn), and (g) biphenyl moiety signal (MeBP; m/z = 168). (a) and (b) Reproduced (adapted) with permission from Ref. [60], © The Royal Society of Chemistry 2010. (c) Adapted with permission from Ref. [61], © Elsevier Science B.V. 2002. (d)–(g) Adapted with permission from Ref. [62], © WILEY-VCH Verlag GmbH & Co. KGaA, Weinheim 2011.

(24 h) into the solution of hexadecanethiol (HDT) or hexadecanselenol (HDSe), respectively, and the residual content of the original molecules was monitored by IR spectroscopy. According to the results (Figs. 10(a) and 10(b)), the denser packed and better oriented SAMs with n = odd are more robust and resistent to the exchange reaction.

The next example refers to electrochemical stability. Within the respective experiments, the MeBPnS SAMs on Au(111) were subjected to adsorption/desorption cycles controlled by cyclovoltammetry [61]. The respective desorption peak potential exhibited pronounced odd-even behavior, being consistenly lower (by ~ 83 mV; in terms of the absolute value) for n = even compared with n = odd (Fig. 10(c)). Thus, the electrochemical stability of the more densely packed and more upright oriented SAMs with n = odd is higher than that of their counterparts with n = even.

A further example is the stability of the MeBPnS SAMs on Au(111) towards ion irradiation, recorded by static secondary neutral mass spectroscopy (S-SNMS) and illustrated in Figs. 10(d)–10(g) [62]. Accordingly, the total yield of molecular material emitted from these films during 15 keV Ar^+ ion irradiation exhibits distinct odd-even behavior, with smaller yield for the denser packed and better ordered SAMs with n = odd compared to their counterparts with n = even (Fig. 10(d)). The odd-even behaviour is also visible in the emission of the complete molecule (MeBPnS, Fig. 10(e)) as well as its fragments corresponding to the desulfurized molecule (MeBPn, Fig. 10(f)) or methyl-biphenyl moiety (MeBP; m/z = 168, Fig. 10(g)). Specifically, the lower MeBPnS emission for n = odd (Fig. 10(e)) indicates higher Au–S bond stability compared to n = even, which is consistent with the odd-even effects discussed above, i.e. the chemical exchange process (Fig. 10(a)) and the electrochemical stability (Fig. 10(c)) as well as with an odd-even variation of the characteristic binding energy of the anchoring groups observed in the high-resolution XPS spectra [28, 33]. Moreover, the reverse phase of the odd-even effects observed for the MeBPn emission (Fig. 10(f)) indicates that increased stability of the Au–S bond for n = odd is achieved at the cost of reduced stability of the neighbouring S–C bond in these SAMs [62]. The odd-even effect for MeBP (Fig. 10(g)) also correlates with the odd-even reorientation of the biphenyl moiety as discussed earlier (Fig. 3) indicating an odd-even stability of the C–C bond linking this moiety to the rest of the aliphatic chain.

Finaly, we note that odd-even behaviour towards ion irradiation was also observed in static secondary ion mass spectroscopy (S-SIMS) analysis of M_2Au^- and M_2Ag^- (M = complete molecule) clusters emitted from MeBPnS and MeBPnSe SAMs on Au(111) and Ag(111), which shows a reversed ´phase´ upon changing the substrate from Au(111) to Ag(111), in accordance with all structural odd-even effects observed for these monolayers [63].

8 Overview of the odd-even data

Whereas most of the published results related to the structure and properties of the aryl-substituted aliphatic SAMs were discussed in the previous sections, we think that a short overview of all relevant publications on this subject (to the best of our knowledge) would be useful. Such an overview is presented in Table 1, along with the parameters of the SAMs and the major goals of the respective studies.

9 Applications of the odd-even behavior

The distinct odd-even behavior of aryl-substituted aliphatic SAMs has a variety of practical implications. First, as discussed in section 7, it provides a practical means to tune properties of these films in context of a specific application. Second, it allows for rational design of aromatic and hybrid aromatic-aliphatic SAMs. As mentioned in several places above, including the discussion of the data presented in Fig. 9, the introduction of a suitable aliphatic linker between the anchoring group and an aryl backbone allows to improve the quality of an aromatic SAM significantly, in terms of both packing density and orientational order. Most frequently, this approach is applied to aromatic SAMs on Au(111) with just a single methylene group (n = odd) as the linker.

A representative example is provided in Fig. 11. The issue was to form a well-defined and stable metal film on a SAM template, which allow for manufacturing of ultrathin insulation layers in electronic and spintronic devices. For this purpose, SAM-forming 1,1',4',1"-terphenyl-4,4"-dimethanethiol (TPDMT) was designed, featuring a terphenyl backbone, methylene linkers, and terminal thiol groups (Fig. 11(a)) [69]. TPDMT formed monolayers of very

Table 1 List of the publications dealing with the odd-even effects in aryl-$(CH_2)_n$-AG SAMs on Au(111), Ag(111), and GaAs(001)[a]

Aryl	*n*	AG	Substrate	Issue	Ref.
Phenyl, biphenyl	0, 1	–S	Au	Structure	[19]
Terphenyl	1	–S	Au	Structure conductance	[20]
Phenyl	1–3	–S	Au	Structure	[64]
Phenyl	12–15	–S	Au	Basic properties	[24]
Methyl-biphenyl	3–6	–S	Au and Ag	Basic properties	[16]
Methyl-biphenyl	1–6	–S	Au and Ag	Basic properties	[17]
Methyl-biphenyl	1–6	–S	Au and Ag	Photoemission	[28]
Methyl-biphenyl	1–6	–S	Au	Electrochemistry	[61]
Methyl-biphenyl	0, 1, 4, 5, 12	–S	Au	Electron irradiation	[57]
Methyl-biphenyl	3 and 4	–S	Au	Structure	[26]
Methyl-biphenyl	1–6	–S	Au	Structure	[27]
Methyl-biphenyl	4	–S	Au	Polymorphism	[53]
Methyl-biphenyl	2, 3, 5	–S	Au	Stress	[65]
Methyl-biphenyl	1–6, 12	–S	Au	Electrochemical stability	[66]
Methyl-biphenyl	4 and 6	–S	Au	Polymorphism, force balance	[32]
Methyl-biphenyl	2	–S	Au	Polymorphism	[67]
Methyl-biphenyl	2, 4, 6	–S	Au	Polymorphism, ion irradiation	[68]
Methyl-biphenyl	2–6	–S	Au	Stability against exchange	[60]
Methyl-biphenyl	1–6	–S	Au	Ion-induced desorption	[62]
Methyl-biphenyl	2–6	–S	Au and Ag	Stability	[63]
Methyl-biphenyl	1–6	–S	GaAs(001)	Basic properties	[51]
Cyano-biphenyl	1, 2	–S	Au	Orientation	[40]
Cyano-biphenyl	0, 1, 2	–S	Au	Basic properties, electron transfer	[41]
Biphenyl	0–6	–S	Au	Theory: structure, properties	[34]
Terphenyl	1–6	–S	Au and Ag	Basic properties	[35]
Terphenyl	1–6	–S	Au	Structure	[36]
Terphenyl	1–6	–S	Au and Ag	Photoemission	[33]
Terphenyl	0–6	–S	GaAs(001)	Basic properties	[49]
Perfluoroterphenyl	2 and 3	–S	Au and Ag	Basic properties	[37]
2-Anthracene (nonsymmetric)	1–6, 10–12	–S	Au and Ag	Basic properties	[52]
Perfluoroanthracene	2 and 3	–S	Au	Basic properties	[39]
Anthraceneoxazole (symmetric)	2–6	–S	Au and Ag	Basic properties	[38]
Azobenzene	3 and 4	–S	Au and Ag	Basic properties	[42]
Methyl-biphenyl	2–6	–Se	Au and Ag	Basic properties	[43]
Methyl-biphenyl	1–6, 10, 11	–Se	Au and Ag	Basic properties	[45]
Methyl-biphenyl	2–6	–Se	Au	Structure	[44]
Methyl-biphenyl	2–6	–Se	Au	Polymorphism	[54]
Methyl-biphenyl	2–6	–Se	Au	Stability against exchange	[60]
Methyl-biphenyl	2–6	–Se	Au and Ag	Stability	[63]
Biphenyl	1–4	–COO	Ag	Basic properties	[55]
Biphenyl	2–6	–COO	Ag	Electron irradiation	[58]

[a]AG is the anchoring group. "Basic properties" include molecular organization, packing density, molecular orientation, etc.

high quality on Au(111), which, after additional electron-induced crosslinking (CL), provided a suitable template for the metal (Ni) deposition. This was verified by ion scattering spectroscopy (ISS) and angular resolved XPS. The Ni and Au ISS profiles taken across the Ni/CL-TPDMT/Au sample show a well-localized Ni film on top of the SAM and no Ni atoms in the SAM and at the SAM/Au interface (Fig. 11(b)). The intensity of the Ni 2p XPS signal does not show any significant variation with the takeoff angle of the photoelectrons, in contrast to the intensity of the C 1s signal from the SAM, which exhibits strong variation (Fig. 11(c)). Such a behavior is characteristic of a well-defined Ni film on the top of the SAM (Fig. 11(d)), in full agreement with the ISS data.

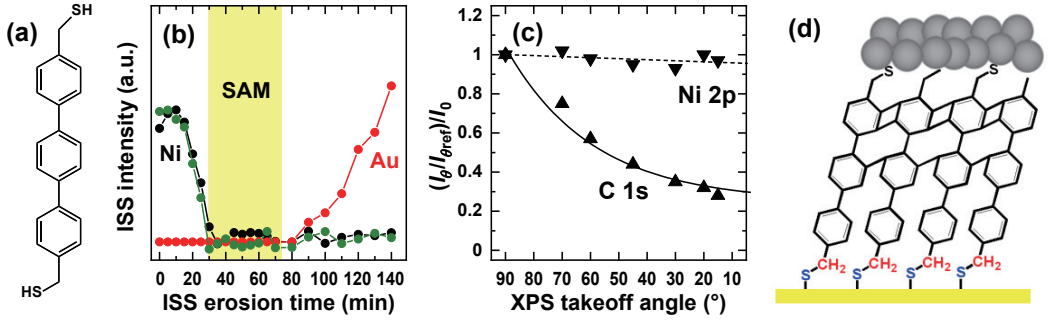

Figure 11 (a) Custom-designed, SAM-forming TPDMT molecule. (b) Intensity of the Ni and Au ISS signals acquired in the course of ion-induced erosion of the Ni/CL-TPDMT/Au sample. (c) Dependence of the normalized intensity of the Ni 2p and C 1s XPS signals on the takeoff angle of the photoelectrons (measured with respect to the substrate surface) for this sample. (d) Schematic of the Ni/CL-TPDMT/Au sample. Adapted with permission from Ref. [69], © WILEY-VCH Verlag GmbH & Co. KGaA, Weinheim 2005.

A further representative example is provided in Fig. 12. The goal of this particular project was to decouple the SAM-induced electrostatic effects from chemical properties of the SAM surface, which in many applications becomes interface to other materials, such as semiconductors. For the electrostatic engineering, which is crucially important in context of energy level alignment in organic electronics and photovoltaics, SAMs are usually decorated with a polar tail group. This, however, changes the chemical identity of the SAM surface, which typically affects the morphology of a functional material deposited on the SAM, such as an organic semiconductor or a buffer layer. The solution is to embed the dipolar group into the molecular chain, which, for the application-relevant aromatic backbone, was for the first time achieved by design of the molecules shown in Fig. 12(a) [70–72]. In these molecules, the central phenylene ring in the terphenyl backbone was replaced by the dipolar pyrimidine group with the dipole moment directed either from or toward the substrate. To obtain densely packed and highly oriented SAMs on Au(111), it was decided to inset a methylene linker (n = odd) between the aromatic part and the anchoring thiol group. The work function of the SAM-modified surface varied then in accordance with the direction of the embedded dipole (Fig. 12(b)) while the chemical identity of this surface, defined by the terminal phenyl ring, remained unchanged. An additional effect is the electrostatic shift of the peak associated with the top phenylene ring in the XPS spectra (Fig. 12(c)), which helped to understand the importance of such effects in photoemission [73] and provided a practical tool to study morphology of dipolar molecular films by XPS [74].

Along with the application-related design of functional, aryl-substituted aliphatic SAMs, pronounced odd-even effects in these systems provide a general tool for SAM design and dedicated studies of specific phenomena associated with molecular self-assembly. The examples of odd-even behavior are odd-even effects in surface wettability, work function, adhesion behavior, tribological properties, electron transfer, and chemical reactivity [18]. A representative example in this regard is given by studies of the effects of in-surface and buried dipoles on the wetting properties of partially fluorinated alkanethiolate SAMs on Au(111) [75–77]. Among other parameters, the length of the alkyl linker was continuously varied and an odd-even variation of the contact angles for different probe liquids was recorded, with a ´phase´ depending on the extent of fluorination and the position of the fluorinated groups in the molecular chain [75–77]. Another example is the effect of the substrate roughness on the morphology and properties of the SAM-ambient interface. Odd-even variation of the contact angle for different probe liquids for a series of non-substituted alkanethiolate SAMs on Ag(111) was considered as a fingerprint of the film morphology and conclusions on acceptable range of surface roughness were drawn [78, 79]. A variety of related effects, associated with the identity of the probe liquids, was recorded and rationalized and useful conclusions regarding interplay of the surface roughness, backbone length, and probe liquid polarity were made.

A further example is design and characterization of ferrocene-functionalized SAMs in context of odd-even effects in the structure and electric conductance properties of thereof [80–82]. On the one hand, these effects were used to optimize inherent packing tendencies of the molecules in the SAMs in order to minimize leakage currents in the two-terminal molecular junctions. On the other hand, it could be demonstrated that the rather moderate odd-even changes in the orientation of the terminal ferrocene group and SAM packing, recorded for these

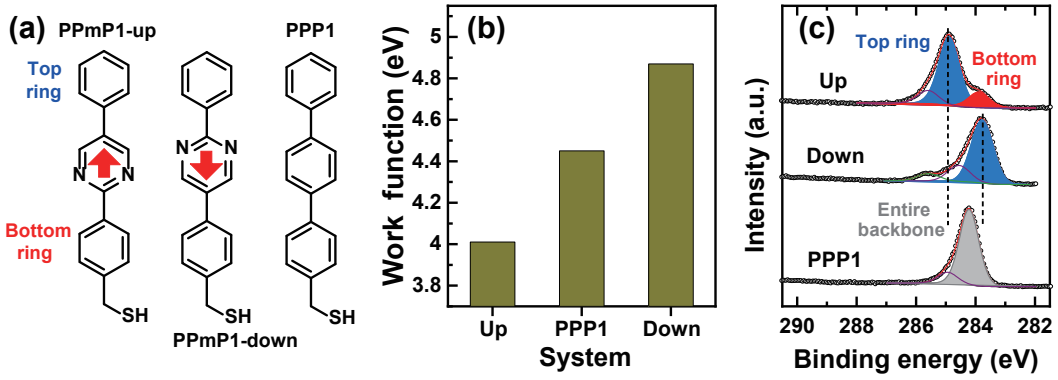

Figure 12 (a) Custom-designed, SAM-forming molecules with embedded dipolar group and the reference, non-polar molecule; (b) work functions of the respective SAMs; and (c) high-resolution XPS spectra of these SAMs acquired at a photon energy of 350 eV. The spectra are decomposed into individual contributions; the peak related to the top ring in the dipolar SAMs shifts depending on the direction of the embedded dipole. Acronyms: P = phenyl, Pm = pyrimidine, 1 = single methylene spacer, up/down = direction of the dipole moment (red arrows) relative to the anchoring group. Adapted with permission from Ref. [70], © WILEY-VCH Verlag GmbH & Co. KGaA, Weinheim 2015.

monolayers, result in significant changes of the electric conductance properties of the SAMs, with a particular strong effect on their rectification ability.

The final example are the experiments on a series of prototypic homo-oligopeptides based on glycine (Gly) with cysteine (Cys) as a substrate bonding group chemisorbed on Au and Ag substrates (Gly_nCys/Au(Ag), n = 1–9) [83]. These monolayers, featuring the –C–S–substrate anchoring motif, exhibit pronounced odd-even structural effects strongly affecting their packing density and molecular conformation. Knowledge and understanding of these effects represent thus a tool for rational design of such monolayers and related biointerfaces.

10 Conclusions

In summary, this review article is devoted to the odd-even effects in the structure and stability of aryl-substituted aliphatic SAMs. On the one hand, these effects are an important phenomenon, providing insight into the delicate balance of the structure-building interactions in monomolecular films. On the other hand, these effects represent a practical tool to vary and to optimize the key parameters of the SAMs such as packing density, molecular orientation, and coupling to the substrate. In its turn, this variation allows to tune the properties of the SAMs, such as their electrochemical stability, stability against exchange by other molecules, reaction to ionizing radiation (electrons, ions), etc. The understanding and rational application of the odd-even effects enable a purpose-specific design of functional SAMs in context of nanofabrication, organic and molecular electronics, and a variety of other practical goals. Because of their general character, odd-even effects are not only limited to aryl-substituted aliphatic SAMs but are also of importance for other aliphatic monolayers, playing an important role in their design and applications.

Acknowledgements

The authors thank their coworkers and cooperation partners around the world, who have contributed to the research described in this review article. M. Z. acknowledges allocation of the beamtimes and valuable technical support during the experiments at BESSY I and BESSY II in Berlin and MAX IV in Lund. P. C. acknowledges the financial support from Alexander von Humboldt Foundation, The Leverhulme Trust, and Foundation for Polish Science. The researches described in this review were financially supported by BMBF, DFG, NSC Poland, and DAAD through a variety of projects.

Funding note: Open Access funding enabled and organized by Projekt DEAL.

References

[1] Schreiber, F. Self-assembled monolayers: From 'simple' model systems to biofunctionalized interfaces. *J. Phys.: Condens. Matter* **2004**, *16*, R881–R900.

[2] Love, J. C.; Estroff, L. A.; Kriebel, J. K.; Nuzzo, R. G.; Whitesides, G. M. Self-assembled monolayers of thiolates on metals as a form of nanotechnology. *Chem. Rev.* **2005**, *105*, 1103–1170.

[3] Kind, M.; Wöll, C. Organic surfaces exposed by self-assembled organothiol monolayers: Preparation, characterization, and application. *Prog. Surf. Sci.* **2009**, *84*, 230–278.

[4] Vericat, C.; Vela, M. E.; Benitez, G.; Carro, P.; Salvarezza, R. C. Self-assembled monolayers of thiols and dithiols on gold: New challenges for a well-known system. *Chem. Soc. Rev.* **2010**, *39*, 1805–1834.

[5] Gooding, J. J.; Ciampi, S. The molecular level modification of surfaces: From self-assembled monolayers to complex molecular assemblies. *Chem. Soc. Rev.* **2011**, *40*, 2704–2718.

[6] Turchanin, A.; Gölzhäuser, A. Carbon nanomembranes. *Adv. Mater.* **2016**, *28*, 6075–6103.

[7] Casalini, S.; Bortolotti, C. A.; Leonardi, F.; Biscarini, F. Self-assembled monolayers in organic electronics. *Chem. Soc. Rev.* **2017**, *46*, 40–71.

[8] Liu, D. Q.; Miao, Q. Recent progress in interface engineering of organic thin film transistors with self-assembled monolayers. *Mater. Chem. Front.* **2018**, *2*, 11–21.

[9] Sizov, A. S.; Agina, E. V.; Ponomarenko, S. A. Self-assembled semiconducting monolayers in organic electronics. *Russ. Chem. Rev.* **2018**, *87*, 1226–1264.

[10] Kong, G. D.; Byeon, S. E.; Park, S.; Song, H.; Kim, S. Y.; Yoon, H. J. Mixed molecular electronics: Tunneling behaviors and applications of mixed self-assembled monolayers. *Adv. Electron. Mater.* **2020**, *6*, 1901157.

[11] Liu, Y. R.; Qiu, X. K.; Soni, S.; Chiechi, R. C. Charge transport through molecular ensembles: Recent progress in molecular electronics. *Chem. Phys. Rev.* **2021**, *2*, 021303.

[12] Telegdi, J. Formation of self-assembled anticorrosion films on different metals. *Materials* **2020**, *13*, 5089.

[13] Terfort, A.; Zharnikov, M. Electron-irradiation promoted exchange reaction as a tool for surface engineering and chemical lithography. *Adv. Mater. Interfaces* **2021**, *8*, 2100148.

[14] Gupta, R.; Fereiro, J. A.; Bayat, A.; Pritam, A.; Zharnikov, M.; Mondal, P. C. Nanoscale molecular rectifiers. *Nat. Rev. Chem.* **2023**, *7*, 106–122.

[15] Schreiber, F. Structure and growth of self-assembling monolayers. *Prog. Surf. Sci.* **2000**, *65*, 151–257.

[16] Zharnikov, M.; Frey, S.; Rong, H.; Yang, Y. J.; Heister, K.; Buck, M.; Grunze, M. The effect of sulfur-metal bonding on the structure of self-assembled monolayers. *Phys. Chem. Chem. Phys.* **2000**, *2*, 3359–3362.

[17] Rong, H. T.; Frey, S.; Yang, Y. J.; Zharnikov, M.; Buck, M.; Wühn, M.; Wöll, C.; Helmchen, G. On the importance of the headgroup substrate bond in thiol monolayers: A study of biphenyl-based thiols on gold and silver. *Langmuir* **2001**, *17*, 1582–1593.

[18] Tao, F.; Bernasek, S. L. Understanding odd-even effects in organic self-assembled monolayers. *Chem. Rev.* **2007**, *107*, 1408–1453.

[19] Tao, Y. T.; Wu, C. C.; Eu, J. Y.; Lin, W. L.; Wu, K. C.; Chen, C. H. Structure evolution of aromatic-derivatized thiol monolayers on evaporated gold. *Langmuir* **1997**, *13*, 4018–4023.

[20] Ishida, T.; Mizutani, W.; Akiba, U.; Umemura, K.; Inoue, A.; Choi, N.; Fujihira, M.; Tokumoto, H. Lateral electrical conduction in organic monolayer. *J. Phys. Chem. B* **1999**, *103*, 1686–1690.

[21] Fuxen, C.; Azzam, W.; Arnold, R.; Witte, G.; Terfort, A.; Wöll, C. Structural characterization of organothiolate adlayers on gold: The case of rigid, aromatic backbones. *Langmuir* **2001**, *17*, 3689–3695.

[22] Ishida, T.; Mizutani, W.; Choi, N.; Akiba, U.; Fujihira, M.; Tokumoto, H. Structural effects on electrical conduction of conjugated molecules studied by scanning tunneling microscopy. *J. Phys. Chem. B* **2000**, *104*, 11680–11688.

[23] Ishida, T.; Mizutani, W.; Tokumoto, H.; Choi, N.; Akiba, U.; Fujihira, M. Insertion process and electrical conduction of

conjugated molecules in n-alkanethiol self-assembled monolayers on Au(111). *J. Vac. Sci. Technol. A* **2000**, *18*, 1437–1442.
[24] Lee, S.; Puck, A.; Graupe, M.; Colorado, R.; Shon, Y. S.; Lee, T. R.; Perry, S. S. Structure, wettability, and frictional properties of phenyl-terminated self-assembled monolayers on gold. *Langmuir* **2001**, *17*, 7364–7370.
[25] Zharnikov, M. Near-edge X-ray absorption fine structure spectroscopy in studies of self-assembled monomolecular films. *J. Electron Spectrosc. Relat. Phenom.* **2023**, *264*, 147322.
[26] Azzam, W.; Cyganik, P.; Witte, G.; Buck, M.; Wöll, C. Pronounced odd-even changes in the molecular arrangement and packing density of biphenyl-based thiol SAMs: A combined STM and LEED study. *Langmuir* **2003**, *19*, 8262–8270.
[27] Cyganik, P.; Buck, M.; Azzam, W.; Wöll, C. Self-assembled monolayers of ω-biphenylalkanethiols on Au(111): Influence of spacer chain on molecular packing. *J. Phys. Chem. B* **2004**, *108*, 4989–4996.
[28] Heister, K.; Rong, H. T.; Buck, M.; Zharnikov, M.; Grunze, M.; Johansson, L. S. O. Odd-even effects at the S-metal interface and in the aromatic matrix of biphenyl-substituted alkanethiol self-assembled monolayers. *J. Phys. Chem. B* **2001**, *105*, 6888–6894.
[29] Laibinis, P. E.; Whitesides, G. M.; Allara, D. L.; Tao, Y. T.; Parikh, A. N.; Nuzzo, R. G. Comparison of the structures and wetting properties of self-assembled monolayers of n-alkanethiols on the coinage metal surfaces, copper, silver, and gold. *J. Am. Chem. Soc.* **1991**, *113*, 7152–7167.
[30] Häkkinen, H. The gold-sulfur interface at the nanoscale. *Nat. Chem.* **2012**, *4*, 443–455.
[31] Forster-Tonigold, K.; Groß, A. A systematic DFT study of substrate reconstruction effects due to thiolate and selenolate adsorption. *Surf. Sci.* **2015**, *640*, 18–24.
[32] Cyganik, P.; Buck, M.; Strunskus, T.; Shaporenko, A.; Wilton-Ely, J. D. E. T.; Zharnikov, M. Wöll, C. Competition as a design concept: Polymorphism in self-assembled monolayers of biphenyl-based thiols. *J. Am. Chem. Soc.* **2006**, *128*, 13868–13878.
[33] Shaporenko, A.; Brunnbauer, M.; Terfort, A.; Johansson, L. S. O.; Grunze, M.; Zharnikov, M. Odd-even effects in photoemission from terphenyl-substituted alkanethiolate self-assembled monolayers. *Langmuir* **2005**, *21*, 4370–4375.
[34] Heimel, G.; Romaner, L.; Brédas, J. L.; Zojer, E. Odd-even effects in self-assembled monolayers of ω-(biphenyl-4-yl)alkanethiols: A first-principles study. *Langmuir* **2008**, *24*, 474–482.
[35] Shaporenko, A.; Brunnbauer, M.; Terfort, A.; Grunze, M.; Zharnikov, M. Structural forces in self-assembled monolayers: Terphenyl-substituted alkanethiols on noble metal substrates. *J. Phys. Chem. B* **2004**, *108*, 14462–14469.
[36] Azzam, W.; Bashir, A.; Terfort, A.; Strunskus, T.; Wöll, C. Combined STM and FTIR characterization of terphenylalkanethiol monolayers on Au(111): Effect of alkyl chain length and deposition temperature. *Langmuir* **2006**, *22*, 3647–3655.
[37] Chesneau, F.; Schüpbach, B.; Szelągowska-Kunstman, K.; Ballav, N.; Cyganik, P.; Terfort, A.; Zharnikov, M. Self-assembled monolayers of perfluoroterphenyl-substituted alkanethiols: Specific characteristics and odd-even effects. *Phys. Chem. Chem. Phys.* **2010**, *12*, 12123–12137.
[38] Partes, C.; Sauter, E.; Gärtner, M.; Kind, M.; Asyuda, A.; Bolte, M.; Zharnikov, M.; Terfort, A. Reestablishing odd-even effects in anthracene-derived monolayers by introduction of a pseudo-C_{2v} symmetry. *J. Phys. Chem. C* **2019**, *123*, 20362–20372.
[39] Zhang, Z. B.; Wächter, T.; Kind, M.; Schuster, S.; Bats, J. W.; Nefedov, A.; Zharnikov, M.; Terfort, A. Self-assembled monolayers of perfluoroanthracenylaminoalkane thiolates on gold as potential electron injection layers. *ACS Appl. Mater. Interfaces* **2016**, *8*, 7308–7319.
[40] Ballav, N.; Schüpbach, B.; Dethloff, O.; Feulner, P.; Terfort, A.; Zharnikov, M. Direct probing molecular twist and tilt in aromatic self-assembled monolayers. *J. Am. Chem. Soc.* **2007**, *129*, 15416–15417.
[41] Ballav, N.; Schüpbach, B.; Neppl, S.; Feulner, P.; Terfort, A.; Zharnikov, M. Biphenylnitrile-based self-assembled monolayers on Au(111): Spectroscopic characterization and resonant excitation of the nitrile tail group. *J. Phys. Chem. C* **2010**, *114*, 12719–12727.
[42] Gnatek, D.; Schuster, S.; Ossowski, J.; Khan, M.; Rysz, J.; Krakert, S.; Terfort, A.; Zharnikov, M.; Cyganik, P. Odd-even effects in the structure and stability of azobenzene-substituted alkanethiolates on Au(111) and Ag(111) substrates. *J. Phys. Chem. C* **2015**, *119*, 25929–25944.
[43] Shaporenko, A.; Müller, J.; Weidner, T.; Terfort, A.; Zharnikov, M. Balance of structure-building forces in selenium-based self-assembled monolayers. *J. Am. Chem. Soc.* **2007**, *129*, 2232–2233.
[44] Cyganik, P.; Szelągowska-Kunstman, K.; Terfort, A.; Zharnikov, M. Odd-even effect in molecular packing of biphenyl-substituted alkaneselenolate self-assembled monolayers on Au(111): Scanning tunneling microscopy study. *J. Phys. Chem. C* **2008**, *112*, 15466–15473.
[45] Weidner, T.; Shaporenko, A.; Müller, J.; Schmid, M.; Cyganik, P.; Terfort, A.; Zharnikov, M. Effect of the bending potential on molecular arrangement in alkaneselenolate self-assembled monolayers. *J. Phys. Chem. C* **2008**, *112*, 12495–12506.
[46] Shaporenko, A.; Cyganik, P.; Buck, M.; Terfort, A.; Zharnikov, M. Self-assembled monolayers of aromatic selenolates on noble metal substrates. *J. Phys. Chem. B* **2005**, *109*, 13630–13638.
[47] Bashir, A.; Käfer, D.; Müller, J.; Wöll, C.; Terfort, A.; Witte, G. Selenium as a key element for highly ordered aromatic self-assembled monolayers. *Angew. Chem., Int. Ed.* **2008**, *47*, 5250–5252.
[48] Ossowski, J.; Wächter, T.; Silies, L.; Kind, M.; Noworolska, A.; Blobner, F.; Gnatek, D.; Rysz, J.; Bolte, M.; Feulner, P. et al. Thiolate versus selenolate: Structure, stability, and charge transfer properties. *ACS Nano* **2015**, *9*, 4508–4526.
[49] Lu, H.; Terfort, A.; Zharnikov, M. Bending potential as an important factor for the structure of monomolecular thiolate layers on GaAs substrates. *J. Phys. Chem. Lett.* **2013**, *4*, 2217–2222.
[50] McGuiness, C. L.; Diehl, G. A.; Blasini, D.; Smilgies, D. M.; Zhu, M.; Samarth, N.; Weidner, T.; Ballav, N.; Zharnikov, M.; Allara, D. L. Molecular self-assembly at bare semiconductor surfaces: Cooperative substrate-molecule effects in octadecanethiolate monolayer assemblies on GaAs(111), (110), and (100). *ACS Nano* **2010**, *4*, 3447–3465
[51] Lu, H.; Zharnikov, M. Structure-building forces in biphenyl-substituted alkanethiolate self-assembled monolayers on GaAs(001): The effect of the bending potential. *J. Phys. Chem. C* **2015**, *119*, 27401–27409.
[52] Dauselt, J.; Zhao, J. L.; Kind, M.; Binder, R.; Bashir, A.; Terfort, A.; Zharnikov, M. Compensation of the odd-even effects in araliphatic self-assembled monolayers by nonsymmetric attachment of the aromatic part. *J. Phys. Chem. C* **2011**, *115*, 2841–2854.
[53] Cyganik, P.; Buck, M. Polymorphism in biphenyl-based self-assembled monolayers of thiols. *J. Am. Chem. Soc.* **2004**, *126*, 5960–5961.
[54] Dendzik, M.; Terfort, A.; Cyganik, P. Odd-even effect in the polymorphism of self-assembled monolayers of biphenyl-substituted alkaneselenolates on Au(111). *J. Phys. Chem. C* **2012**, *116*, 19535–19542.
[55] Krzykawska, A.; Szwed, M.; Ossowski, J.; Cyganik, P. Odd-even effect in molecular packing of self-assembled monolayers of biphenyl-substituted fatty acid on Ag(111). *J. Phys. Chem. C* **2018**, *122*, 919–928.
[56] Zharnikov, M.; Grunze, M. Modification of thiol-derived self-assembling monolayers by electron and X-ray irradiation: Scientific and lithographic aspects. *J. Vac. Sci. Technol. B* **2002**, *20*, 1793–1807.
[57] Frey, S.; Rong, H. T.; Heister, K.; Yang, Y. J.; Buck, M.; Zharnikov, M. Response of biphenyl-substituted alkanethiol self-assembled monolayers to electron irradiation: Damage suppression and odd-even effects. *Langmuir* **2002**, *18*, 3142–3150.
[58] Kruk, M.; Neumann, C.; Frey, M.; Kozieł, K.; Turchanin, A.; Cyganik, P. Odd-even effect in electron beam irradiation of hybrid aromatic-aliphatic self-assembled monolayers of fatty acid. *J. Phys. Chem. C* **2021**, *125*, 9310–9318.
[59] Neumann, C.; Szwed, M.; Frey, M.; Tang, Z. A.; Kozieł, K.; Cyganik, P.; Turchanin, A. Preparation of carbon nanomembranes

without chemically active groups. *ACS Appl. Mater. Interfaces* **2019**, *11*, 31176–31181.
[60] Szelagowska-Kunstman, K.; Cyganik, P.; Schüpbach, B.; Terfort, A. Relative stability of thiol and selenol based SAMs on Au(111)-exchange experiments. *Phys. Chem. Chem. Phys.* **2010**, *12*, 4400–4406.
[61] Long, Y. T.; Rong, H. T.; Buck, M.; Grunze, M. Odd-even effects in the cyclic voltammetry of self-assembled monolayers of biphenyl based thiols. *J. Electroanal. Chem.* **2002**, *524–525*, 62–67
[62] Vervaecke, F.; Wyczawska, S.; Cyganik, P.; Bastiaansen, J.; Postawa, Z.; Silverans, R. E.; Vandeweert, E.; Lievens, P. Odd-even effects in ion-beam-induced desorption of biphenyl-substituted alkanethiol self-assembled monolayers. *ChemPhysChem* **2011**, *12*, 140–144.
[63] Ossowski, J.; Rysz, J.; Terfort, A.; Cyganik, P. Relative stability of thiolate and selenolate SAMs on Ag(111) substrate studied by static SIMS Oscillation in stability of consecutive chemical bonds. *J. Phys. Chem. C* **2017**, *121*, 459–470.
[64] Yang, G. H.; Liu, G. Y. New insights for self-assembled monolayers of organothiols on Au(111) revealed by scanning tunneling microscopy. *J. Phys. Chem. B* **2003**, *107*, 8746–8759.
[65] Cyganik, P.; Buck, M.; Wilton-Ely, J. D. E. T.; Wöll, C. Stress in self-assembled monolayers: ω-biphenyl alkane thiols on Au(111). *J. Phys. Chem. B* **2005**, *109*, 10902–10908.
[66] Thom, I.; Buck, M. Electrochemical stability of self-assembled monolayers of biphenyl based thiols studied by cyclic voltammetry and second harmonic generation. *Surf. Sci.* **2005**, *581*, 33–46.
[67] Cyganik, P.; Buck, M.; Strunskus, T.; Shaporenko, A.; Witte, G.; Zharnikov, M.; Wöll, C. Influence of molecular structure on phase transitions: A study of self-assembled monolayers of 2-(aryl)-ethane thiols. *J. Phys. Chem. C* **2007**, *111*, 16909–16919.
[68] Vervaecke, F.; Wyczawska, S.; Cyganik, P.; Postawa, Z.; Buck, M.; Silverans, R. E.; Lievens, P.; Vandeweert, E. Phase-dependent desorption from biphenyl-substituted alkanethiol self-assembled monolayers induced by ion irradiation. *J. Phys. Chem. C* **2008**, *112*, 2248–2251.
[69] Tai, Y.; Shaporenko, A.; Noda, H.; Grunze, M.; Zharnikov, M. Fabrication of stable metal films on the surface of self-assembled monolayers. *Adv. Mater.* **2005**, *17*, 1745–1749.
[70] Abu-Husein, T.; Schuster, S.; Egger, D. A.; Kind, M.; Santowski, T.; Wiesner, A.; Chiechi, R.; Zojer, E.; Terfort, A.; Zharnikov, M. The effects of embedded dipoles in aromatic self-assembled monolayers. *Adv. Funct. Mater.* **2015**, *25*, 3943–3957.
[71] Petritz, A.; Krammer, M.; Sauter, E.; Gärtner, M.; Nascimbeni, G.; Schrode, B.; Fian, A.; Gold, H.; Cojocaru, A.; Karner-Petritz, E. et al. Embedded dipole self-assembled monolayers for contact resistance tuning in p-type and n-type organic thin film transistors and flexible electronic circuits. *Adv. Funct. Mater.* **2018**, *28*, 1804462.
[72] Zojer, E.; Terfort, A.; Zharnikov, M. Concept of embedded dipoles as a versatile tool for surface engineering. *Acc. Chem. Res.* **2022**, *55*, 1857–1867.
[73] Taucher, T. C.; Hehn, I.; Hofmann, O. T.; Zharnikov, M.; Zojer, E. Understanding chemical versus electrostatic shifts in X-ray photoelectron spectra of organic self-assembled monolayers. *J. Phys. Chem. C* **2016**, *120*, 3428–3437.
[74] Hehn, I.; Schuster, S.; Wächter, T.; Abu-Husein, T.; Terfort, A.; Zharnikov, M.; Zojer, E. Employing X-ray photoelectron spectroscopy for determining layer homogeneity in mixed polar self-assembled monolayers. *J. Phys. Chem. Lett.* **2016**, *7*, 2994–3000.
[75] Zenasni, O.; Marquez, M. D.; Jamison, A. C.; Lee, H. J.; Czader, A.; Lee, T. R. Inverted surface dipoles in fluorinated self-assembled monolayers. *Chem. Mater.* **2015**, *27*, 7433–7446.
[76] Lee, H. J.; Jamison, A. C.; Lee, T. R. Surface dipoles: A growing body of evidence supports their impact and importance. *Acc. Chem. Res.* **2015**, *48*, 3007–3015.
[77] Marquez, M. D.; Zenasni, O.; Rodriguez, D.; Yu, T. L.; Sakunkaewkasem, S.; Toro Figueira, F.; Czader, A.; Baldelli, S.; Lee, T. R. Burying the inverted surface dipole: Self-assembled monolayers derived from alkyl-terminated partially fluorinated alkanethiols. *Chem. Mater.* **2020**, *32*, 953–968.
[78] Wang, Z. J.; Chen, J. H.; Oyola-Reynoso, S.; Thuo, M. Empirical evidence for roughness-dependent limit in observation of odd-even effect in wetting properties of polar liquids on n-alkanethiolate self-assembled monolayers. *Langmuir* **2016**, *32*, 8230–8237.
[79] Du, C. S.; Wang, Z.J.; Chen, J. H.; Martin, A.; Raturi, D.; Thuo, M. Role of nanoscale roughness and polarity in odd-even effect of self-assembled monolayers. *Angew. Chem., Int. Ed.* **2022**, *61*, e202205251.
[80] Yuan, L.; Thompson, D.; Cao, L.; Nerngchangnong, N.; Nijhuis, C. A. One carbon matters: The origin and reversal of odd-even effects in molecular diodes with self-assembled monolayers of ferrocenyl-alkanethiolates. *J. Phys. Chem. C* **2015**, *119*, 17910–17919.
[81] Yuan, L.; Nerngchamnong, N.; Cao, L.; Hamoudi, H.; del Barco, E.; Roemer, M.; Sriramula, R. K.; Thompson, D.; Nijhuis, C. A. Controlling the direction of rectification in a molecular diode. *Nat. Commun.* **2015**, *6*, 6324.
[82] Thompson, D.; Nijhuis, C. A. Even the odd numbers help: Failure modes of SAM-based tunnel junctions probed via odd-even effects revealed in synchrotrons and supercomputers. *Acc. Chem. Res.* **2016**, *49*, 2061–2069.
[83] Grabarek, A.; Walczak, Ł.; Cyganik, P. Odd-even effect in peptide SAMs-competition of secondary structure and molecule-substrate interaction. *J. Phys. Chem. B* **2021**, *125*, 10964–10971.